TITLE: Functional variations in gamma-secretase activity are critical determinants of the clinical, biomarker, and cognitive progression of autosomal dominant Alzheimer's disease

AUTHOR LIST Stephanie A. Schultz, PhD[1], Lei Liu, MD, PhD[2,3], Aaron P. Schultz, PhD[1], Colleen D. Fitzpatrick, MA[1], Raina Levin, BS[1], Jean-Pierre Bellier, PhD[2,3], Zahra Shirzadi, PhD[2,3], Nelly Joseph-Mathurin, PhD[4], Charles D. Chen, PhD[4], Tammie L.S. Benzinger, MD, PhD[4], Gregory S. Day, MD[5], Martin R. Farlow, MD[6], Brian A. Gordon, PhD[4], Jason J. Hassenstab, PhD[4], Clifford R. Jack Jr., MD[7], Mathias Jucker, PhD[8], Celeste M. Karch, PhD[4], Jae-Hong Lee, MD, PhD[9], Johannes Levin, MD[10-12], Richard J. Perrin, MD, PhD[4], Peter R Schofield, PhD, DSc[13,14], Chengjie Xiong, PhD[4], Keith A. Johnson, MD[1,2], Eric McDade, DO[4], Randall J. Bateman, MD[4], Reisa A. Sperling, MD[1,2], Dennis J. Selkoe, MD[2,3], Jasmeer P. Chhatwal, MD, PhD, MMSc*[1,2,3], and the Dominantly Inherited Alzheimer Network Investigators

[1]Massachusetts General Hospital, Harvard Medical School; Boston, MA, USA

[2]Brigham and Women's Hospital; Boston, MA, USA

[3]Ann Romney Center for Neurologic Diseases; Boston, MA, USA

[4]Washington University in St. Louis School of Medicine; St. Louis, MO, USA

[5]Mayo Clinic; Jacksonville, FL, USA

[6]Indiana Alzheimer's Disease Research Center; Indianapolis, IN, USA

[7]Mayo Clinic, Rochester; MN, USA

[8]German Center for Neurodegenerative Diseases (DZNE); Tuebingen, Germany

[9]Asan Medical Center, University of Ulsan College of Medicine; Seoul, Korea

[10]German Center for Neurodegenerative Diseases (DZNE); Munich, Germany

[11]Department of Neurology, Ludwig-Maximilians-Universität München; Munich, Germany

[12]Munich Cluster for Systems Neurology (SyNergy); Munich, Germany

[13]Neuroscience Research Australia; Randwick, NSW, Australia

[14]School of Medical Sciences, University of New South Wales; Sydney, NSW, Australia

*Corresponding author: Jasmeer P. Chhatwal MD, PhD, MMSc; Email: Chhatwal.Jasmeer@mgh.harvard.edu

ABSTRACT

Background: The balance between production, clearance, and toxicity of Aβ peptides is central to Alzheimer's disease (AD) pathobiology. Though highly variable in terms of age at symptom onset (AAO), hundreds of variants in *PSEN1* cause autosomal dominant forms of AD (ADAD) with nearly complete penetrance. PSEN1 forms the catalytic core of the γ-secretase complex and thereby directly mediates the production of longer, aggregation-prone Aβ peptides relative to shorter, non-aggregating peptides. We hypothesized that the broad AAO and biomarker heterogeneity seen across ADAD would be predictable based on mutation-specific differences in the production of Aβ species.

Methods: Aβ-37, 38, 40, 42, and 43 production was quantified from 162 unique *PSEN1* variants expressed in HEK293 cells. Prediction of AAO was carried out in 107 variants with available AAO and then replicated in 55 variants represented across 190 PSEN1 mutation carriers who have detailed cognitive and biomarker data from the Dominantly Inherited Alzheimer's Network (DIAN).

Results: Variations in Aβ production across the 162 mutations examined in cell-based models were highly predictive of AAO. In those with corresponding *in vivo* data from the DIAN study, our cell-based γ-secretase composite was strongly associated with biomarker and cognitive trajectories.

Conclusions: These findings elucidate the critical link between γ-secretase function, Aβ production, and AD progression and offer mechanistic support for the amyloid hypothesis. The approach used here represents a powerful tool to account for heterogeneity in disease progression in ADAD clinical trials and to assess the pathogenicity of variants of unknown significance or with limited family history.

INTRODUCTION

An increase in longer, aggregation-prone Aβ fragments (e.g., Aβ 42 and 43) relative to shorter, non-aggregating fragments (e.g., Aβ 37 and 38) is a critical initiating pathogenic event in both late-onset, sporadic AD[1] (LOAD) and Autosomal Dominant AD[2–4] (ADAD). The balance between production of aggregating and non-aggregating forms of Aβ is a direct result of the efficiency and kinetics with which the γ-secretase proteolytic complex sequentially cleaves β-amyloid precursor protein[5–9] (APP). Subtle alterations in γ-secretase function can lead to profound neurodegenerative and cognitive consequences, while modulation of γ-secretase has therapeutic potential in both LOAD and ADAD[8–12]. Over 200 pathogenic variants in *Presenilin-1* (*PSEN1*), the key catalytic subunit in the γ-secretase complex, have been identified and are the most common causes of ADAD[13]. Mirroring the heterogeneity in clinical and AD biomarker progression seen in LOAD, there is striking heterogeneity in age of symptom onset (AAO)[14–16] and rates of cognitive and biomarker change[17–21] across carriers of *PSEN1* pathogenic variants. We hypothesized that this heterogeneity may be strongly tied to underlying mutation-level variation in γ-secretase function.

Intriguingly, prior work suggests some pathogenic *PSEN1* variants may not significantly alter the absolute amounts of Aβ42 production[22], indicating that more thorough investigation is needed to understand how these pathogenic variants lead to ADAD and the mechanisms that cause earlier vs. later disease onset and progression. To this end, findings from our group[23] and others[24] suggest that probing the ratios of short-to-long Aβ peptide production across ADAD pathogenic variants may help us understand the observed heterogeneity in these populations.

98 Here, we leverage a live-cell-based model system and newly developed
99 immunoassays to functionally characterize APP processing by γ-secretase across a
100 large set of *PSEN1* pathogenic variants with AAOs ranging from the 20s to the 70s. We
101 then assess how this mutation-level characterization of γ-secretase function may
102 explain heterogeneity in neuroimaging and biofluid biomarkers, as well as clinical
103 measures among *PSEN1* carriers with available data from the Dominantly Inherited
104 Alzheimer's Network Observational Study (DIAN-Obs).
105

106 **METHODS**

107 **Functional assays of γ-secretase function**

108 162 unique *PSEN1* variants, including 55 unique variants represented in DIAN-Obs and
109 data from 107 unique variants previously characterized in Liu et al., 2022,[23] and wild-
110 type (normal) *PSEN1* was characterized for Aβ peptide production and γ-secretase
111 function. Using methods detailed in supplemental methods and a prior report using this
112 model system, each *PSEN1* variant or normal *PSEN1* was sub-cloned and placed into
113 the PcDNA 3.1 expression vector[23]. Subsequently, each variant was co-transfected with
114 a plasmid encoding wild-type (normal) human APP-C99 into HEK293T cells genetically
115 depleted of *PSEN1* and *PSEN2*[23]. Creation of this cell line and transient transfection
116 procedures are described in supplemental methods. Conditioned media from
117 transfected HEK cells was harvested and diluted with 1% BSA in wash buffer (TBS
118 supplemented with 0.05% Tween). Aβ37, 38, 40, 42, and 43 immunoassays were
119 performed in triplicate and averaged as previously described[23] (see Figure S1 and
120 supplemental methods). Absolute peptide production levels and relevant ratios were

121 examined as percent relative to the production seen in the same model system
122 following transfection with normal (wild-type) *PSEN1.*
123
124 **Participants**
125 Participants provided written informed consent prior to the completion of any study
126 procedures, in accordance with Institution Review Board policy at each participating
127 site. Data were included from 190 *PSEN1* pathogenic variant carriers enrolled in DIAN-
128 Obs, each carrying one of 55 unique *PSEN1* pathogenic variants characterized via cell-
129 based methods (see Figure 1A, Table S1, and Table S2). Detailed protocols for DIAN
130 have previously been published and are described in supplemental methods. For DIAN-
131 Obs participants, the familial AAO was determined through structured interviews to
132 determine the age of onset of progressive cognitive decline for the participant's first
133 degree relative(s)[15].
134 Clinical evaluators were blind to the mutation status of participants. Participants
135 underwent comprehensive clinical and cognitive evaluations. Clinical Dementia Rating
136 (CDR®) Sum of Boxes (SB) was assessed for each participant using structured
137 interviews, as previously described[25]. Mini-Mental State Examination (MMSE) and
138 Wechsler Memory Scale-Revised Logical Memory Delayed Recall[26] were selected a
139 priori as our cognitive measures of interest. All DIAN-Obs participants with available Aβ
140 positron emission tomography (PET), magnetic resonance imaging (MRI), and at least
141 one cognitive assessment were included (Figure 1A; DIAN-Obs data freeze version 15;
142 last data from June 30, 2020; see supplemental methods). A subset of these individuals
143 also had [^{18}F]Fluorodeoxyglucose (FDG)-PET (n=162) and cerebrospinal fluid (CSF)

144 (n=157) available for analyses. Longitudinal data were available from 154 DIAN
145 participants (Table S3). For the 107 *PSEN1* variants studies previously in Liu et al.
146 (non-overlapping with the 55 variants from DIAN-Obs), AAO was derived from prior
147 literature, as previously described[23].
148
149 **Imaging and Fluid Biomarker Analyses**
150 Protocols for Aβ and brain metabolism PET, MRI, and CSF studies are described in
151 detail in supplemental methods and in previously published work[21,25,27–31]. Cerebral Aβ
152 load was measured using [^{11}C]Pittsburgh Compound B (PiB) PET, and brain glucose
153 metabolism was measured with [^{18}F]FDG-PET. Partial volume corrected values were
154 used in all analyses. FreeSurfer v 5.3 defined regional measures were derived from MRI
155 data. CSF Aβ42, Aβ40, and phosphorylated-tau181 levels were measured using an
156 automated immunoassay system (LUMIPULSE G1200, Fujirebio, Malvern, PA).
157 Phosphorylated-tau 217 (pT217/T217) values were derived from immunoprecipitation-
158 mass spectrometry (IP-MS) as previously described[27]. See supplemental methods for
159 additional details.
160
161 **Statistical Analyses**
162 Analyses were conducted using R (version 4.0.3, R Foundation for Statistical
163 Computing). Pearson correlations were used to assess associations of Aβ production
164 and γ-secretase function with AAO. A summary measure of variant-level Aβ production
165 and γ-secretase function (γ-secretase composite) was developed to reduce the number

of statistical comparisons and facilitate comparisons between mutant and wild-type *PSEN1*, as described in the Results.

Linear mixed effect models including fixed effects for age, sex, and γ-secretase composite score were employed to assess associations between the cell-based γ-secretase function and multi-modal biomarker and clinical data from DIAN. Similar to prior work from DIAN, a random effect for family membership was included in each linear mixed effects model. Separate models were used to assess associations with each clinical, cognitive, or biomarker outcome measure, focusing on CSF Aβ 42/40, CSF phosphorylated-tau 181, CSF phosphorylated-tau 217, hippocampal volume, CDR-SB, MMSE, and logical memory delayed (see supplemental methods). Years of education was included as an additional fixed effect term in models examining cognitive and clinical outcomes. Longitudinal models were similarly constructed but additionally included interactions of each fixed effect with time and terms allowing both a random intercept and slope. Additional exploratory analyses made use of a tertile split of γ-secretase composite scores to visualize how clinical, cognitive, and biomarker trajectories can be understood in the context of γ-secretase function.

RESULTS

Cell-based measures of γ-secretase function are associated with age of symptom onset.

Aβ 37, 38, 40, 42, and 43 production was assessed in 162 unique *PSEN1* variants, including 55 *PSEN1* variants represented in DIAN (Table S1) and 107

190 non-overlapping variants previously characterized in Liu et al., 2022[23]. Grouping
191 together Aβ production for all 162 variants, we observed reductions in Aβ37, 38, and 40
192 compared to normal levels (median % reduction relative to normal = -56.8, -48.6, and -
193 22.8%, respectively), suggesting that, as a group, *PSEN1* pathogenic variants decrease
194 the processive γ-cleavage of Aβ by γ-secretase (γ-processivity), leading to a decrease in
195 these fully processed (shorter) Aβ peptides. Additionally, relative levels of Aβ42 and 43
196 across variants were higher in *PSEN1* pathogenic variants compared to normal levels
197 (median % increase relative to normal= 66.5% and 47.1%; respectively).

198 We first assessed relationships between the relative concentrations of Aβ
199 species produced by each variant and AAO in a set of 107 variants not represented in
200 the DIAN study. To limit comparisons with multiple ratios when assessing relationships
201 between γ-secretase function and AAO, we leveraged prior literature[1,23,24,32,33]
202 suggesting the Aβ 42/40 ratio and a measure of the efficiency of successive cleavage
203 (γ-processivity) of Aβ fragments can be used to summarize γ-secretase function. These
204 two measures were operationalized as $\log_{10}(\frac{\text{A}\beta42}{\text{A}\beta40})$ (a measure of the relative production
205 of aggregation-prone Aβ) and a ratio of short (fully γ-secretase processed) to long
206 (incompletely γ-secretase processed) Aβ fragments ($\frac{\text{short A}\beta37+38}{\text{long A}\beta42+43}$). As expected, $\frac{\text{A}\beta42}{\text{A}\beta40}$,
207 and $\frac{\text{short A}\beta37+38}{\text{long A}\beta42+43}$ ratio levels across *PSEN1* pathogenic variants were both abnormal
208 (decreased processivity) compared to normal levels (median % change relative to the
209 normal = 108.9 and -71.3%). In the initial sample of 107 *PSEN1* pathogenic variants
210 from Liu et al., both higher $\log_{10}(\frac{\text{A}\beta42}{\text{A}\beta40})$ (r[105] = -0.64, p = 2.20e-13) and lower

211 $\frac{\text{short A}\beta37+38}{\text{long A}\beta42+43}$ (r[105] = 0.66, p =2.28e-14) levels were associated with earlier AAO (Figure
212 1B-C). Both ratios remained significantly associated when entered together into a single
213 model predicting AAO (Table S4), suggesting that they capture unique variance with
214 respect to the pathogenicity of each variant. Accordingly, these two ratios were
215 combined into a single summary measure of variant-level γ-secretase function (γ –
216 secretase $Composite = \frac{short\ A\beta37+38}{long\ A\beta42+43} - log_{10}\frac{A\beta42}{A\beta40}$). To facilitate visualization and
217 comparison, the γ-secretase composite is expressed as a percentage of wild-type γ-
218 secretase function.

219 In both the subset of variants represented in the DIAN-Obs and remaining
220 variants characterized previously by Liu et al[23], γ-secretase composite scores were
221 lower in all pathogenic variants compared to normal (average of 60.4% reduction
222 relative to normal). The γ-secretase composite had a the highest degree of correlation
223 with AAO (Liu et al cohort: r[105] = 0.71, p <2.2e-16; DIAN-Obs cohort: r[53] = 0.61, p =
224 6.10e-07; Figure 1E), as compared to using individual Aβ peptide levels, $\frac{\text{A}\beta42}{\text{A}\beta40}$ levels, or
225 $\frac{\text{short A}\beta37+38}{\text{long A}\beta42+43}$ ratio levels in the initial set of 107 *PSEN1* variants and in the 55 variants
226 represented in DIAN (see above). To demonstrate the potential utility of using the γ-
227 secretase composite to predict an approximate AAO for novel pathogenic variants
228 and/or when a clinical history is not available, we list the γ-secretase composite derived
229 AAO (AAO_{gsc}) values for the 55 DIAN-Obs variants examined here (Table S1). Notably,
230 γ-secretase composite values did not map in a straightforward manner onto the location
231 of the corresponding pathogenic variant within *PSEN1*, and substantial variation within a

232 single codon in terms of gamma-secretase function was observed for several sites in
233 which more than one variant was characterized (Table S1; Figure 1D).
234
235 **Lower cell-based γ-secretase composite scores are associated with more**
236 **abnormal AD imaging and fluid biomarkers.**
237 Lower γ-secretase composite scores (decreased γ-secretase function relative to
238 normal) were associated with higher levels of mean cortical Aβ burden (B[SE] = -
239 0.03[0.01], p =4.06e-07; Figure 2A) as assessed by Aβ PET, after controlling for
240 demographic factors. Exploratory regional analyses revealed widespread associations
241 between *in vivo* Aβ burden and the cell-based γ-secretase composite, with the strongest
242 associations seen in the precuneus, and anterior and posterior cingulate (Figure 2D).
243 We next examined associations between the variant-level γ-secretase composite
244 and commonly used imaging biomarkers of neurodegeneration, including structural MRI
245 and FDG-PET, in DIAN-Obs participants carrying one of the 55 of the *PSEN1* variants
246 characterized *in vitro*. Both the MRI-based measures hippocampal volume (B[SE] =
247 44.22[6.4], p = 5.15e-10; Figure 2B) and precuneus FDG-PET signal (B[SE] =
248 0.006[0.001], p = 5.38e-05; Figure 2C) were highly associated with the γ-secretase
249 composite, after controlling for demographic factors. Exploratory regional analyses
250 revealed that the cell-based γ-secretase composite significantly accounted for
251 widespread grey matter volume differences across *PSEN1* variant carriers, most
252 notably in the hippocampus, amygdala, temporal regions, precuneus, and posterior
253 cingulate (Figure 2E), as well as differences in glucose metabolism including the
254 precuneus, parietal, and frontal regions (Figure 2F).

255 Using established CSF measures of AD pathology, we observed that lower
256 variant-specific γ-secretase composite scores were associated with lower CSF Aβ 42/40
257 (B[SE] = 6.3e-04[1.5e-04], p = 4.46e-05; Figure 3A), higher CSF ELISA
258 log_{10}(phosphorylated-tauT181) levels (B[SE] = -0.009[0.002], p =4.47e-06; Figure 3B),
259 and higher CSF IP-MS log_{10}(pT217/T217) levels (B[SE] = -0.01[0.002], p =1.98e-05;
260 Figure 3C).
261
262 **γ-secretase composite scores are associated with clinical and cognitive measures**
263 **in *PSEN1* pathogenic variant carriers in DIAN-Obs.**
264 The cell-derived γ-secretase composite levels predicted changes of MMSE
265 (B[SE] = 0.11[.03], p = 2.17e-04; Figure 3D), CDR-SB (B[SE] = -0.07[0.02], p = 4.86e-
266 05; Figure 3E), and logical memory-delayed scores (B[SE] = 0.11[.03], p = 6.51e-05;
267 Figure 3F).
268
269 **γ-secretase composite scores predict rate of change in biomarker, clinical and**
270 **cognitive features in *PSEN1* ADAD carriers.**
271 We next assessed how longitudinal rates of change in core biomarker, clinical,
272 and cognitive measures of interest (Figure 4A, C, E, and G) may be related to cell-
273 based measures of γ-secretase function. Lower (more pathogenic) γ-secretase
274 composite measures were associated with faster increase in β-amyloid PET signal
275 (B[SE] = -7.2e-04[2e-04], p = 0.003; Figure 4B), as well as more rapid decreases in
276 hippocampal volume (B[SE] = 4.56[0.7], p = 2.96e-10; Figure 4D), MMSE (B[SE] =

277 0.02[0.007], p = 3.02e-04; Figure 4F), and logical memory-delayed (B[SE] =
278 0.006[0.001], p = 2.63e-06; Figure 4H).
279
280 **Multimodal models suggest variant level variations in γ-secretase function may**
281 **impact the clinical, cognitive, and biomarker progression of ADAD.**
282 To assess how differences in γ-secretase function may alter the observed
283 clinical, cognitive, and biomarker course of ADAD, we performed a tertile split of
284 variants represented in DIAN and plotted the standardized change in core clinical,
285 cognitive, and biomarker measures across the lifespan for individuals carrying *PSEN1*
286 pathogenic mutations in the lowest, middle, or highest tertile of γ-secretase function
287 (Figure 5A-C). To complement this group-level analysis, we used all available data to
288 visualize putative disease trajectories for carriers of 2 hypothetical variants with 25%
289 and 75% of normal γ-secretase function, respectively (Figure 5D-I). Consistent with the
290 foregoing analyses, these visualizations demonstrate an earlier shift in AAO, clinical and
291 biomarker abnormalities in carriers of variants with lower (more pathogenic) γ-secretase
292 composite scores. A similar pattern was seen when using estimated years to symptom
293 onset (EYO; calculated by subtracting history-derived AAO from the participant's age)
294 rather than age (Figure S2A-B). This suggests that cell-based assessments of γ-
295 secretase add to the prediction of disease trajectories even after history-derived
296 information about AAO is included in statistical models. However, while a shift in the
297 timing of symptom and biomarker changes was seen across a range of γ-secretase
298 function, it is notable that elevations in pathological Aβ burden (higher Aβ PET or lower
299 CSF Aβ42) and tau (higher CSF phosphorylated-tau181) appear to be early events

300 across all tertiles and precede changes in neurodegenerative markers (hippocampal
301 volume, FDG PET) and clinical measures of impairment (CDR-SB). Together, these
302 results suggest that, while mutation-level variations in γ-secretase function may impact
303 the age of symptom onset and rate of ADAD progression, the ordering of clinical,
304 cognitive, and biomarker changes is not itself fundamentally altered by differences in γ-
305 secretase function.
306
307 **DISCUSSION:**
308 The study of ADAD forms a cornerstone for understanding AD pathobiology, informing
309 the development of new AD biomarkers, broadly influencing the design of animal
310 models of AD, and advancing therapeutic approaches for both LOAD and ADAD. While
311 ADAD-causing *PSEN1* pathogenic variants are highly penetrant, remarkable
312 heterogeneity in the AAO, rates of disease progression, and biomarker changes is seen
313 across variants. Here we examined whether variant level differences in γ-secretase
314 processing of APP may be critical determinants of the age at which *PSEN1* pathogenic
315 variant carriers manifest cognitive changes and develop abnormalities in core
316 biomarkers for AD. Using a cell-based model system to assess the production of a
317 broad set of Aβ peptides, we observed that mutation level differences in γ-secretase
318 processing of APP strongly predicted the age at which progressive cognitive symptoms
319 are manifest (AAO) for a given variant. In addition to predicting AAO, we observed that
320 a summary measure of γ-secretase function was associated with the rates of functional
321 (CDR-SB) and cognitive decline. This composite measure of γ-secretase function was
322 also associated with all fluid and imaging biomarker measures of AD pathobiology and

323 neurodegeneration we examined, including CSF measures of AD pathology, Aβ PET,
324 FDG-PET, and MRI gray matter volumes. These results suggest that accounting for
325 mutation-level γ-secretase dysfunction may clarify treatment effects in ADAD clinical
326 trials and may also be useful in predicting approximate AAO and disease trajectories for
327 *PSEN1* pathogenic variants that are novel or lack sufficient clinical history.
328 Mechanistically, these results highlight the direct importance of γ-secretase function to
329 AD pathobiology and provide support for γ-secretase modulation as a potentially
330 powerful AD therapeutic and preventative strategy[34].

331 Using a human cell-based model system, we found substantial variability in the
332 production of shorter (Aβ-37 and 38) to longer (Aβ-42 and 43) Aβ peptides across a
333 large number of *PSEN1* pathogenic variants. In this same system, we observed that the
334 Aβ42/40 ratio was increased in a majority but not all variants examined. We first
335 examined 107 *PSEN1* variants with available AAO but no available clinical and
336 biomarker data and observed that both the ratio of short-to-long Aβ peptide production
337 ($\frac{\text{Aβ37+38}}{\text{Aβ42+43}}$) and the more commonly used Aβ 42/40 ratio were predictive of AAO.
338 Intriguingly, each of these ratios was independently associated with AAO, and a
339 composite measure derived from these two ratios provided stronger associations with
340 AAO than either alone. This composite measure was carried forward to examine AD
341 progression in a non-overlapping set of *PSEN1* carriers with available clinical and
342 biomarker measures of AD progression.

343 We found that the γ-secretase composite measure explained substantial
344 biomarker heterogeneity across *PSEN1* pathogenic mutation carriers using available
345 data from DIAN. Focusing on associations between the γ-secretase composite and Aβ

346 PET, we observed that individuals who carried pathogenic variants in the lowest (most
347 pathogenic) tertile had, on average, 1.4 SUVR units greater Aβ PET signal compared to
348 those with variants in the highest (least pathogenic) tertile, after accounting for age and
349 sex. Putting these differences in the context of the conventionally used threshold for Aβ
350 PET positivity in this cohort and with this Aβ PET tracer (cortical PiB PET SUVR positive
351 at >= 1.42 SUVR[28]), carriers of pathogenic variants in the lowest (most pathogenic)
352 tertile of the γ-secretase composite would, on average, become amyloid positive ~15
353 years sooner than those carrying *PSEN1* variants in the highest (least pathogenic)
354 tertile (estimated mean age of 22.6 and 37.2 years for low and high tertiles,
355 respectively). Consistent with cross-sectional results, analysis of longitudinal data
356 demonstrated that Aβ PET signal increased more quickly in individuals carrying *PSEN1*
357 variants with lower (more pathogenic) γ-secretase composite scores compared to those
358 with higher composite scores. Though further work is needed to elucidate regional
359 differences, the results here also suggest that variants with low γ-secretase composite
360 values may have greater striatal Aβ PET signal compared to carriers of *PSEN1* variants
361 with high composite values.

362 Cerebrospinal fluid measures of AD pathology also had significant associations
363 with the variant-level γ-secretase composite, including CSF measures of Aβ42/40 and
364 phosphorylated-tau181, and phosphorylated-tau217. In addition to associations with
365 core measures of AD pathobiology, γ-secretase composite scores correlated with FDG
366 PET and structural MRI, two commonly used neuroimaging measures of
367 neurodegeneration. Together with the described associations with AAO and functional
368 impairment measures, this broad pattern of association between γ-secretase function

369 with core AD and neurodegenerative markers further support the hypothesis that
370 heterogeneity in ADAD can broadly be understood in the context of mutation-level
371 differences in γ-secretase dysfunction. Importantly, despite variations in AAO and
372 biomarker trajectories across variants, the results here also support prior observations
373 that pathologic changes in Aβ and tau consistently precede neurodegenerative changes
374 and clinical impairment across *PSEN1* variants[23,24,35]. Additionally, as the γ-secretase
375 composite used here was derived to predict AAO, it remains quite possible that different
376 formulations of this summary measure of γ-secretase function will be better optimized to
377 predict particular biomarker trajectories in clinical trial settings.

378 The results here need to be considered in the context of certain limitations.
379 Though AAO information was available on all *PSEN1* variants examined, only a subset
380 had available clinical, cognitive, and biomarker data from the DIAN-Obs study.
381 Accordingly, data from new pathogenic variants in DIAN and in the broader scientific
382 literature will need to be considered. Similarly, tau PET data will need to be considered
383 in future analyses as they become available. Further, it will be important to determine if
384 processing of γ-secretase substrates besides APP is additionally informative for
385 understanding the differential pathogenicity across *PSEN1* variants. Lastly, it will be
386 critical to extend the cell-based model system to allow for the characterization of
387 pathogenic variants in *PSEN2* and *APP*, as ~20% of ADAD-causing variants are found
388 within these genes.

389 Despite these limitations, these findings indicate that variant level differences in
390 γ-secretase function are highly associated with core measures of clinical, biomarker,
391 and cognitive, progression of ADAD, and suggest that these variant-level differences

392 explain a large portion of the heterogeneity seen across *PSEN1* pathogenic mutation
393 carriers. As the biochemical measures of γ-secretase function used here are derived
394 outside the context of family polygenic factors, age, and estimated years to symptom
395 onset, they offer a potentially unique channel of information with respect to disease
396 progression compared to these other factors and may thus represent useful
397 complements to these measures in ADAD clinical trials. Similarly, as these cell-based
398 measures are divorced from family polygenic factors and age, they may prove to be
399 valuable in gauging the impact of genetic and lifestyle factors that may confer resilience
400 or risk for ADAD onset and progression. Cell-based measures of γ-secretase function
401 may be particularly useful to assess pathogenicity, potential AAO, and predicted AD
402 trajectories for newly discovered *PSEN1* pathogenic variants or for variants lacking
403 sufficient clinical history. Importantly, these results also strongly support the continued
404 investigation of γ-secretase modulators as an AD therapeutic strategy. Lastly, by
405 demonstrating a tight linkage between the processing of APP by γ-secretase in a cell-
406 based model system and ADAD disease trajectories *in vivo*, the results here provide
407 strong support for the hypothesis that dysregulation of APP processing is central to AD
408 pathogenesis, offing support for some formulations of the "Aβ hypothesis" of AD
409 pathogenesis.
410

411 **AUTHORS' CONFLICT OF INTERESTS**

412 Partial funding from the Alzheimer's Association (SAS), NIH grants (CRJ, GSD, JMN,
413 JCM, RJB, TLSB, JPC), NIA grants (GSD), GHR Foundation (CRJ), Alexander Family
414 Alzheimer's Disease Research Professorship of Mayo Clinic (CRJ), grants from Lilly

(NGR), Biogen (NGR), AbbVie (NGR, JL), Chan-Zuckerberg Initiative (GSD), DZNE (JL), Eisai (CR), Instituto de Salud Carlos III (RSV), Anonymous Foundation (PRS).

Consultations have been declared for Humana Healthcare (JPC), Roche (NCF, JL, CR, RSV, RJB), Biogen (NCF, JL, CR), Parabon Nanolabs Inc. (GSD), DynaMed (EBSCO Health) (GSD), medical testimony on legal cases pertaining to management of Wernicke Encephalopathy (GSD), MODAG (JL), GmbH (JL), Bayer Vital (JL), Axon Neuroscience (JL), Thieme Medical Publishers (JL), Prothena (CR), Wave Pharmaceuticals (RSV), Janssen (RSV), Neuraxpharm (RSV), Eisai (RJB), and Amgen (RJB). Other financial interests include owning stocks greater than $10000 are held in ANI Pharmaceuticals (GSD), being a member of the DIAN-TU Pharma Consortium which includes funding and non-financial support for the DIAN-TU-001 trial from Avid Radiopharmaceuticals, Janssen Hoffman Roche/Genentech, Eli Lilly & Co, Eisai, Biogen, AbbVie, and Bristol Meyer Squibbs (RJB, TLSB), and royalties from C2N Diagnostics with equity ownership interest (RJB).

Non-financial interests include serving on an independent data monitoring board for Roche (CRJ), support from Lilly (NCF), support from Ionis (NCF), serving as director of Anti- NMDA Receptor Encephalitis Foundation (GSD), Eisai (TLSB), Siemens (TLSB), and a member of speaker's bureau for Biogen (TLSB).

All other authors have nothing to disclose.

ACKNOWLEDGMENTS:

Data collection and sharing for this project was supported by the Dominantly Inherited Alzheimer Network (DIAN, U19AG032438) funded by the National Institute on Aging (NIA), the Alzheimer's Association (SG-20-690363-DIAN), the German Center for Neurodegenerative Diseases (DZNE), Raul Carrea Institute for Neurological Research (FLENI). Partial support by the Research and Development Grants for Dementia from Japan Agency for Medical Research and Development, AMED, and the Korea Health Technology R&D Project through Korea Health Industry Development Institute (KHIDI), Spanish Institute of Health Carlos III (ISCIII), Canadian Institutes of Health Research (CIHR), Canadian Consortium of Neurodegeneration and Aging, Brain Canada Foundation and Fonds de Recherche du Québec – Santé. This manuscript has been reviewed by DIAN Study investigators for scientific content and consistency of data interpretation with previous DIAN Study publications. We acknowledge the altruism of the participants and their families, and contributions of the DIAN research and support staff at each of the participating sites for their contributions to this study.

452 **REFERENCES:**

453 1. Lagomarsino VN, Pearse RV, Liu L, et al. Stem cell-derived neurons reflect features
454 of protein networks, neuropathology, and cognitive outcome of their aged human
455 donors. *Neuron*. 2021;109(21):3402-3420.e9. doi:10.1016/j.neuron.2021.08.003

456 2. Hsu S, Gordon BA, Hornbeck R, et al. Discovery and validation of autosomal
457 dominant Alzheimer's disease mutations. *Alz Res Therapy*. 2018;10(1):67.
458 doi:10.1186/s13195-018-0392-9

459 3. Karch CM, Hernández D, Wang JC, et al. Human fibroblast and stem cell resource
460 from the Dominantly Inherited Alzheimer Network. *Alzheimers Res Ther*.
461 2018;10(1):69. doi:10.1186/s13195-018-0400-0

462 4. Lanoiselée HM, Nicolas G, Wallon D, et al. APP, PSEN1, and PSEN2 mutations in
463 early-onset Alzheimer disease: A genetic screening study of familial and sporadic
464 cases. *PLoS Med*. 2017;14(3):e1002270. doi:10.1371/journal.pmed.1002270

465 5. De Strooper B, Iwatsubo T, Wolfe MS. Presenilins and γ-secretase: structure,
466 function, and role in Alzheimer Disease. *Cold Spring Harb Perspect Med*.
467 2012;2(1):a006304. doi:10.1101/cshperspect.a006304

468 6. Fernandez MA, Klutkowski JA, Freret T, Wolfe MS. Alzheimer presenilin-1 mutations
469 dramatically reduce trimming of long amyloid β-peptides (Aβ) by γ-secretase to
470 increase 42-to-40-residue Aβ. *J Biol Chem*. 2014;289(45):31043-31052.
471 doi:10.1074/jbc.M114.581165

472 7. Liu L, Lauro BM, Wolfe MS, Selkoe DJ. Hydrophilic loop 1 of Presenilin-1 and the
473 APP GxxxG transmembrane motif regulate γ-secretase function in generating
474 Alzheimer-causing Aβ peptides. *Journal of Biological Chemistry*. 2021;296:100393.
475 doi:10.1016/j.jbc.2021.100393

476 8. Wolfe MS. Dysfunctional γ-Secretase in Familial Alzheimer's Disease. *Neurochem*
477 *Res*. 2019;44(1):5-11. doi:10.1007/s11064-018-2511-1

478 9. Wolfe MS, Selkoe DJ. Giving Alzheimer's the old one-two. *Cell*. 2010;142(2):194-
479 196. doi:10.1016/j.cell.2010.07.006

480 10. Wolfe MS. Probing Mechanisms and Therapeutic Potential of γ-Secretase in
481 Alzheimer's Disease. *Molecules*. 2021;26(2):E388. doi:10.3390/molecules26020388

482 11. Nie P, Vartak A, Li YM. γ-Secretase inhibitors and modulators: Mechanistic insights
483 into the function and regulation of γ-Secretase. *Semin Cell Dev Biol*. 2020;105:43-
484 53. doi:10.1016/j.semcdb.2020.03.002

485 12. Raven F, Ward JF, Zoltowska KM, et al. Soluble Gamma-secretase Modulators
486 Attenuate Alzheimer's β-amyloid Pathology and Induce Conformational Changes in
487 Presenilin 1. *EBioMedicine*. 2017;24:93-101. doi:10.1016/j.ebiom.2017.08.028

13. *Psen-1| Alzforum. (n.d.). Retrieved August 09, 2021, from Https://Www.Alzforum.Org/Mutations/Psen-1*.

14. Ryan NS, Nicholas JM, Weston PSJ, et al. Clinical phenotype and genetic associations in autosomal dominant familial Alzheimer's disease: a case series. *The Lancet Neurology*. 2016;15(13):1326-1335. doi:10.1016/S1474-4422(16)30193-4

15. Ryman DC, Acosta-Baena N, Aisen PS, et al. Symptom onset in autosomal dominant Alzheimer disease: a systematic review and meta-analysis. *Neurology*. 2014;83(3):253-260.

16. Lippa CF, Swearer JM, Kane KJ, et al. Familial Alzheimer's disease: site of mutation influences clinical phenotype. *Ann Neurol*. 2000;48(3):376-379.

17. Wegiel J, Wisniewski HM, Kuchna I, et al. Cell-Type-Specific Enhancement of Amyloid-β Deposition in a Novel Presenilin-1 Mutation (P117L): *Journal of Neuropathology and Experimental Neurology*. 1998;57(9):831-838. doi:10.1097/00005072-199809000-00004

18. Klunk WE, Price JC, Mathis CA, et al. Amyloid Deposition Begins in the Striatum of Presenilin-1 Mutation Carriers from Two Unrelated Pedigrees. *Journal of Neuroscience*. 2007;27(23):6174-6184. doi:10.1523/JNEUROSCI.0730-07.2007

19. Tang M, Ryman DC, McDade E, et al. Neurological manifestations of autosomal dominant familial Alzheimer's disease: a comparison of the published literature with the Dominantly Inherited Alzheimer Network observational study (DIAN-OBS). *The Lancet Neurology*. 2016;15(13):1317-1325.

20. Ryan NS, Rossor MN. Correlating familial Alzheimer's disease gene mutations with clinical phenotype. *Biomarkers Med*. 2010;4(1):99-112. doi:10.2217/bmm.09.92

21. Chhatwal JP, Schultz SA, McDade E, et al. Variant-dependent heterogeneity in amyloid β burden in autosomal dominant Alzheimer's disease: cross-sectional and longitudinal analyses of an observational study. *Lancet Neurol*. 2022;21(2):140-152. doi:10.1016/S1474-4422(21)00375-6

22. Kumar-Singh S, Theuns J, Van Broeck B, et al. Mean age-of-onset of familial alzheimer disease caused by presenilin mutations correlates with both increased Aβ42 and decreased Aβ40. *Hum Mutat*. 2006;27(7):686-695. doi:10.1002/humu.20336

23. Liu L, Lauro BM, He A, et al. Identification of the Aβ37/42 peptide ratio in CSF as an improved Aβ biomarker for Alzheimer's disease. *Alzheimers Dement*. Published online March 12, 2022. doi:10.1002/alz.12646

24. Petit D, Fernández SG, Zoltowska KM, et al. Aβ profiles generated by Alzheimer's disease causing PSEN1 variants determine the pathogenicity of the mutation and

524 predict age at disease onset. *Mol Psychiatry*. 2022;27(6):2821-2832.
525 doi:10.1038/s41380-022-01518-6

526 25. Bateman RJ, Xiong C, Benzinger TLS, et al. Clinical and Biomarker Changes in
527 Dominantly Inherited Alzheimer's Disease. *New England Journal of Medicine*.
528 2012;367(9):795-804. doi:10.1056/NEJMoa1202753

529 26. Wechsler D. Wechsler Memory Scale (3rd ed.): Administration and scoring manual.
530 Published online 1997.

531 27. Barthélemy NR, Li Y, Joseph-Mathurin N, et al. A soluble phosphorylated tau
532 signature links tau, amyloid and the evolution of stages of dominantly inherited
533 Alzheimer's disease. *Nat Med*. 2020;26(3):398-407. doi:10.1038/s41591-020-0781-z

534 28. Su Y, D'Angelo GM, Vlassenko AG, et al. Quantitative Analysis of PiB-PET with
535 FreeSurfer ROIs. *PLOS ONE*. 2013;8(11):e73377.
536 doi:10.1371/journal.pone.0073377

537 29. Su Y, Blazey TM, Owen CJ, et al. Quantitative Amyloid Imaging in Autosomal
538 Dominant Alzheimer's Disease: Results from the DIAN Study Group. *PLoS One*.
539 2016;11(3):e0152082. doi:10.1371/journal.pone.0152082

540 30. Gordon BA, Blazey TM, Su Y, et al. Spatial patterns of neuroimaging biomarker
541 change in individuals from families with autosomal dominant Alzheimer's disease: a
542 longitudinal study. *The Lancet Neurology*. 2018;17(3):241-250.

543 31. McKay NS, Gordon BA, Hornbeck RC, et al. *Neuroimaging within the Dominantly*
544 *Inherited Alzheimer's Network (DIAN): PET and MRI*. Neuroscience; 2022.
545 doi:10.1101/2022.03.25.485799

546 32. Gu L, Guo Z. Alzheimer's Aβ42 and Aβ40 peptides form interlaced amyloid fibrils. *J*
547 *Neurochem*. 2013;126(3):305-311. doi:10.1111/jnc.12202

548 33. Cullen N, Janelidze S, Palmqvist S, et al. Association of CSF Aβ38 Levels With Risk
549 of Alzheimer Disease-Related Decline. *Neurology*. 2022;98(9):e958-e967.
550 doi:10.1212/WNL.0000000000013228

551 34. Toyn JH, Boy KM, Raybon J, et al. Robust Translation of -Secretase Modulator
552 Pharmacology across Preclinical Species and Human Subjects. *Journal of*
553 *Pharmacology and Experimental Therapeutics*. 2016;358(1):125-137.
554 doi:10.1124/jpet.116.232249

555 35. Sun L, Zhou R, Yang G, Shi Y. Analysis of 138 pathogenic mutations in presenilin-1
556 on the in vitro production of Aβ42 and Aβ40 peptides by γ-secretase. *Proc Natl Acad*
557 *Sci U S A*. 2017;114(4):E476-E485. doi:10.1073/pnas.1618657114

558

559 **TABLES AND FIGURES**

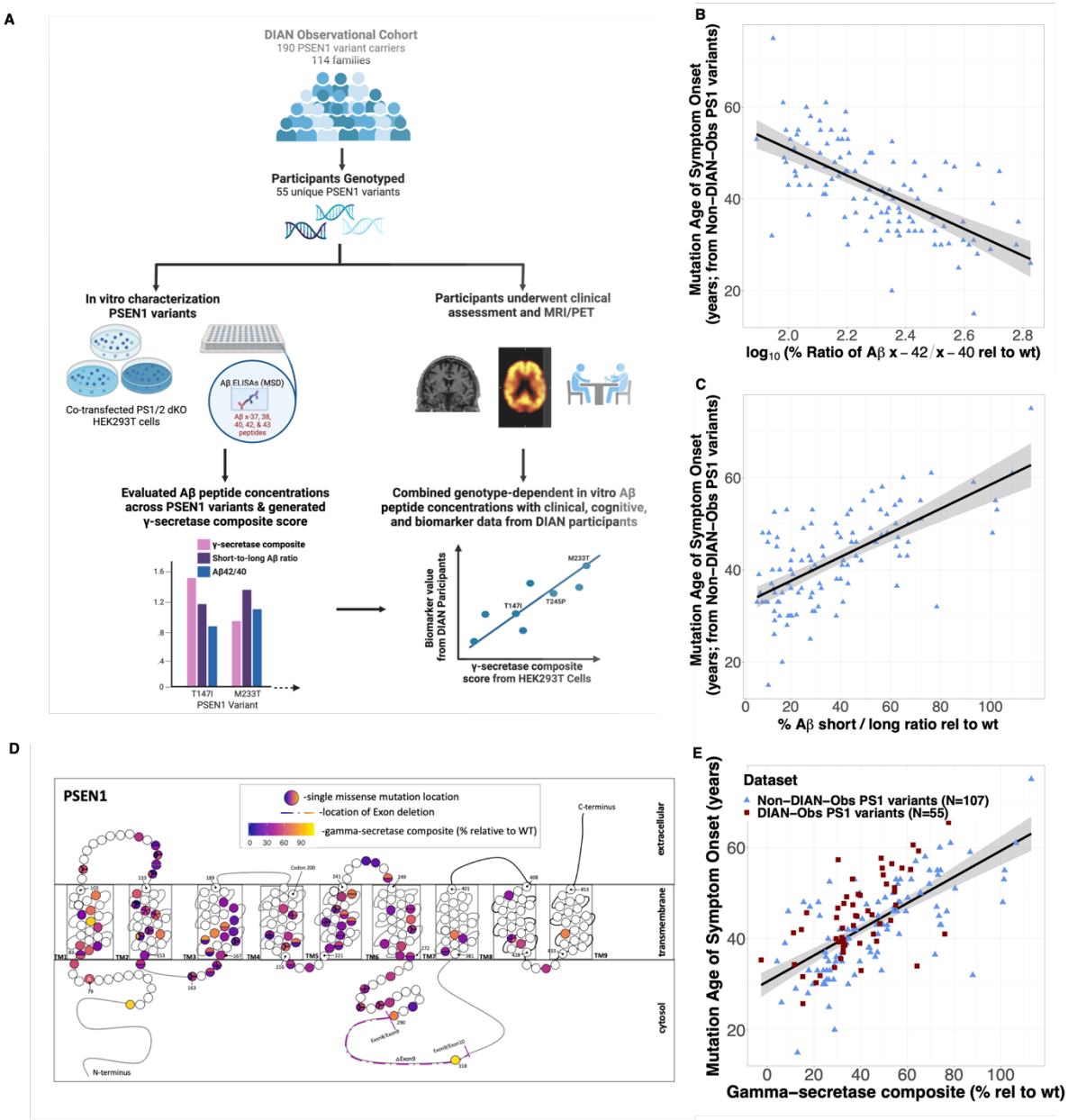

560

561 **Figure 1. Cell-based measures of γ-secretase function are tightly associated with**
562 **age of symptom onset across two cohorts representing 162 unique *PSEN1***
563 **variants. (A)** Schematic summarizing the characterization of variant-level γ-secretase
564 function and correlations with age of symptom onset, cognitive, and biomarker data for
565 each variant (created with BioRender.com). γ-secretase function was summarized using
566 two ratios of Aβ peptide production derived from cell models (**B**) Cell-based $\log_{10}(\frac{\text{A}\beta42}{\text{A}\beta40})$
567 levels and (**C**) a ratio of short (fully γ-secretase processed) to long (incompletely γ-
568 secretase processed) Aβ fragments ($\frac{\text{short A}\beta37+38}{\text{long A}\beta42+43}$) . Both ratios were independently
569 associated with age of symptom onset in an initial set of 107 *PSEN1* variants (B-C). To
570 reduce comparisons going forward, both ratios were combined into a single composite

measure (γ-secretase composite, expressed as a percentage of normal γ-secretase function; D). This composite measure correlated with age of symptom onset in both the initial set of 107 *PSEN1* variants and in a second set of 55 *PSEN1* variants represented in DIAN-Obs (E). Individual data points are jittered to maintain blinding.

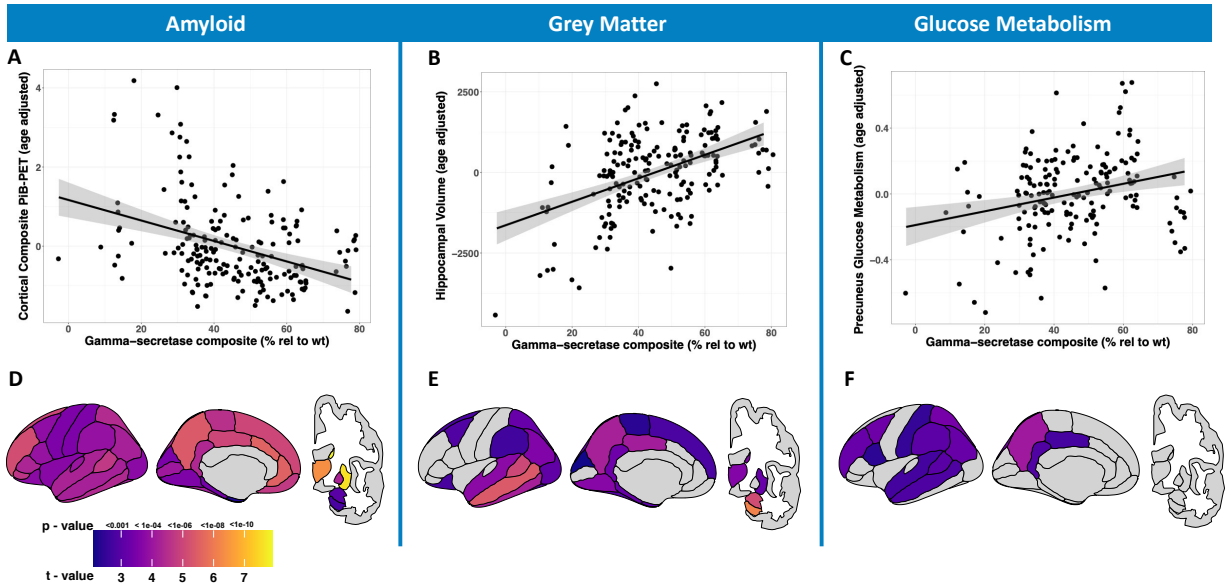

Figure 2. Lower γ-secretase function across variants is associated with more abnormal AD imaging biomarkers. Association between variant-level γ-secretase function and in *vivo* imaging biomarker data from carriers of corresponding *PSEN1* pathogenic variants is shown for cross-sectional Aβ PET (age-adjusted PiB-PET SUVR cortical composite, **A**), age- and intracranial volume-adjusted bilateral hippocampal grey matter volume derived from structural MRI (**B**), and age-adjusted bilateral precuneus FDG-PET SUVR (**C**) from 190 *PSEN1* pathogenic variant carriers (55 unique variants represented). Individual data points are jittered to maintain blinding of the data. Exploratory, regional analyses comparing PiB-PET SUVRs (**D**), grey matter volumes (**E**), and FDG-PET SUVRs (**F**) across a range of γ-secretase function, with colors indicating t- and p-values derived from the comparison of neuroimaging data from *PSEN1* carriers with variants in the lowest (most pathogenic) vs. highest (least pathogenic) tertiles of γ-secretase composite function. Models additionally adjusted for age and sex. Individual data points are jittered to maintain blinding.

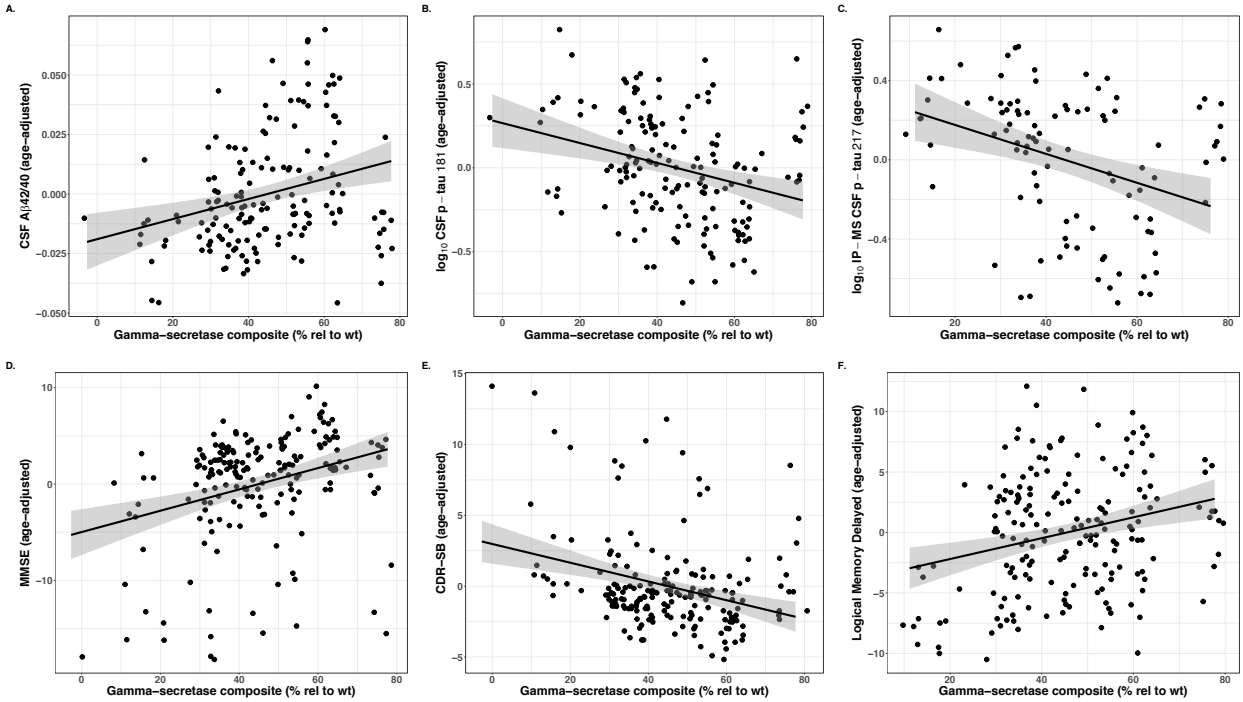

Figure 3. Lower γ-secretase function across variants is associated with more abnormal biofluid, clinical, and cognitive measures in ADAD. Associations between γ-secretase function for each *PSEN1* variant and cross-sectional CSF Aβ 42/40 (**A**), age-adjusted CSF $\log_{10}$ pT181 (**B**), CSF $\log_{10}$ pT217/T217 (**C**), age-adjusted MMSE (**D**), age-adjusted CDR-SB (**E**), and age-adjusted logical memory-delayed (**F**) values from 190 *PSEN1* pathogenic variant carriers (55 unique variants represented) are shown. Individual data points are jittered to maintain blinding.

CSF = Cerebrospinal Fluid; pT = phosphorylated tau; MMSE = Mini Mental State Examination scores; CDR-SB = Clinical Dementia Rating Scale- Sum of Boxes.

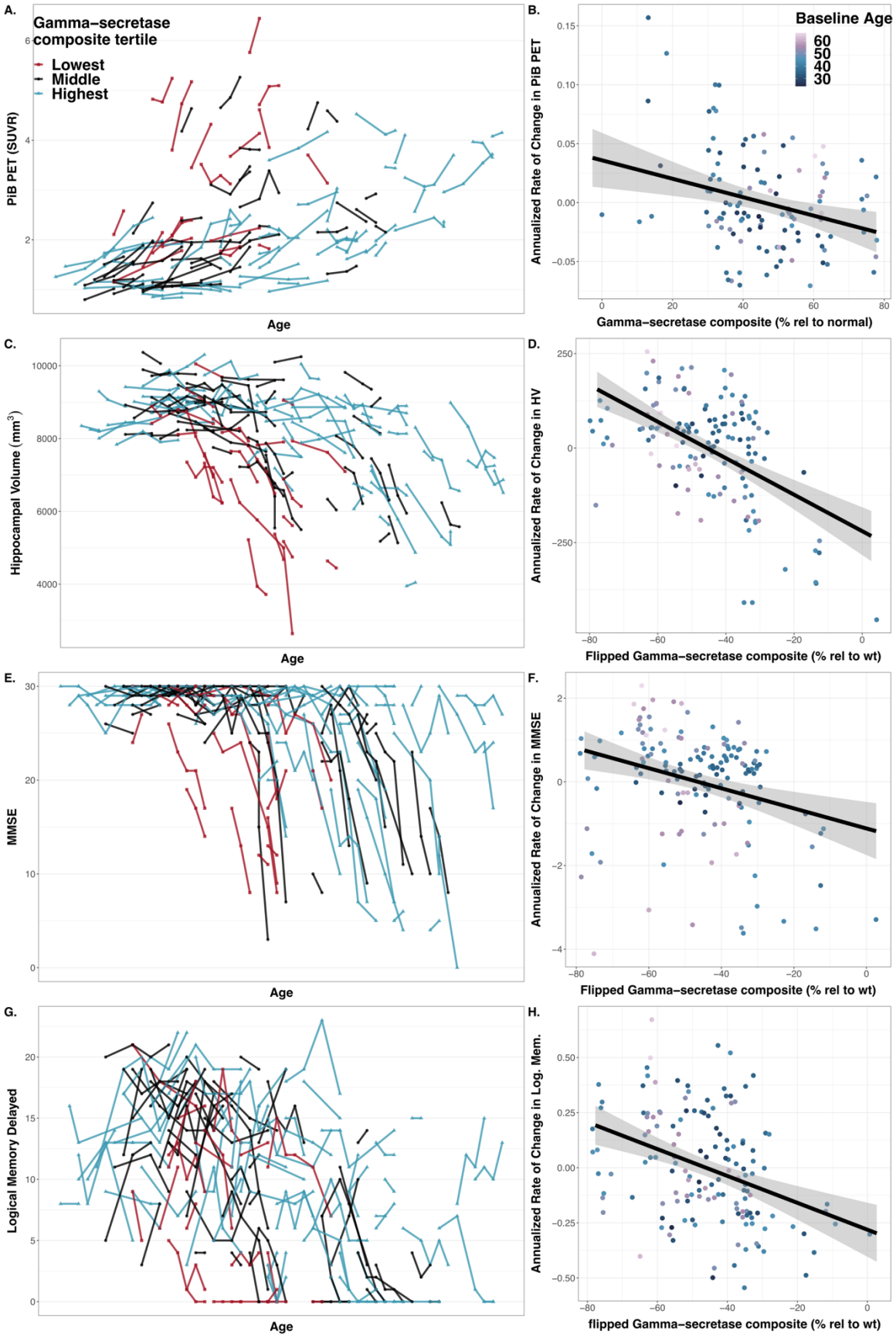
A.
Gamma−secretase composite tertile
Lowest
Middle
Highest
PiB PET (SUVR)
Age
B.
Baseline Age
60
50
40
30
Annualized Rate of Change in PiB PET
Gamma−secretase composite (% rel to normal)
C.
Hippocampal Volume (mm3)
Age
D.
Annualized Rate of Change in HV
Flipped Gamma−secretase composite (% rel to wt)
E.
MMSE
Age
F.
Annualized Rate of Change in MMSE
Flipped Gamma−secretase composite (% rel to wt)
G.
Logical Memory Delayed
Age
H.
Annualized Rate of Change in Log. Mem.
flipped Gamma−secretase composite (% rel to wt)

603

604 **Figure 4. Lower γ-secretase function across *PSEN1* variants is associated with**
605 **more rapid worsening in biomarker, clinical and cognitive measures in ADAD.**
606 Individual longitudinal measures are plotted for PiB-PET SUVR (Aβ burden; **A**),
607 hippocampal volume (HV; mm^3; **C**), Mini Mental Status Exam (MMSE; **E**), and logical
608 memory delayed (Log. Mem.; **G**). Colors indicate whether an individual's *PSEN1* variant
609 is in the low (red; most pathogenic tertile), middle (black; intermediate pathogenicity), or
610 high (blue; least pathogenic) tertile for γ-secretase function. To facilitate statistical
611 comparison, age-adjusted, individual-level slopes for each biomarker and cognitive
612 outcomes of interest were extracted from linear mixed effects models and plotted
613 against γ-secretase function (Aβ PET – **B**; Hippocampal Volume – **D**; MMSE – **F**;
614 Logical Memory – **H**). Significant associations were observed between rate-of-change
615 in each measure and variant-level γ-secretase function. Individual data points are
616 jittered to maintain blinding.
617

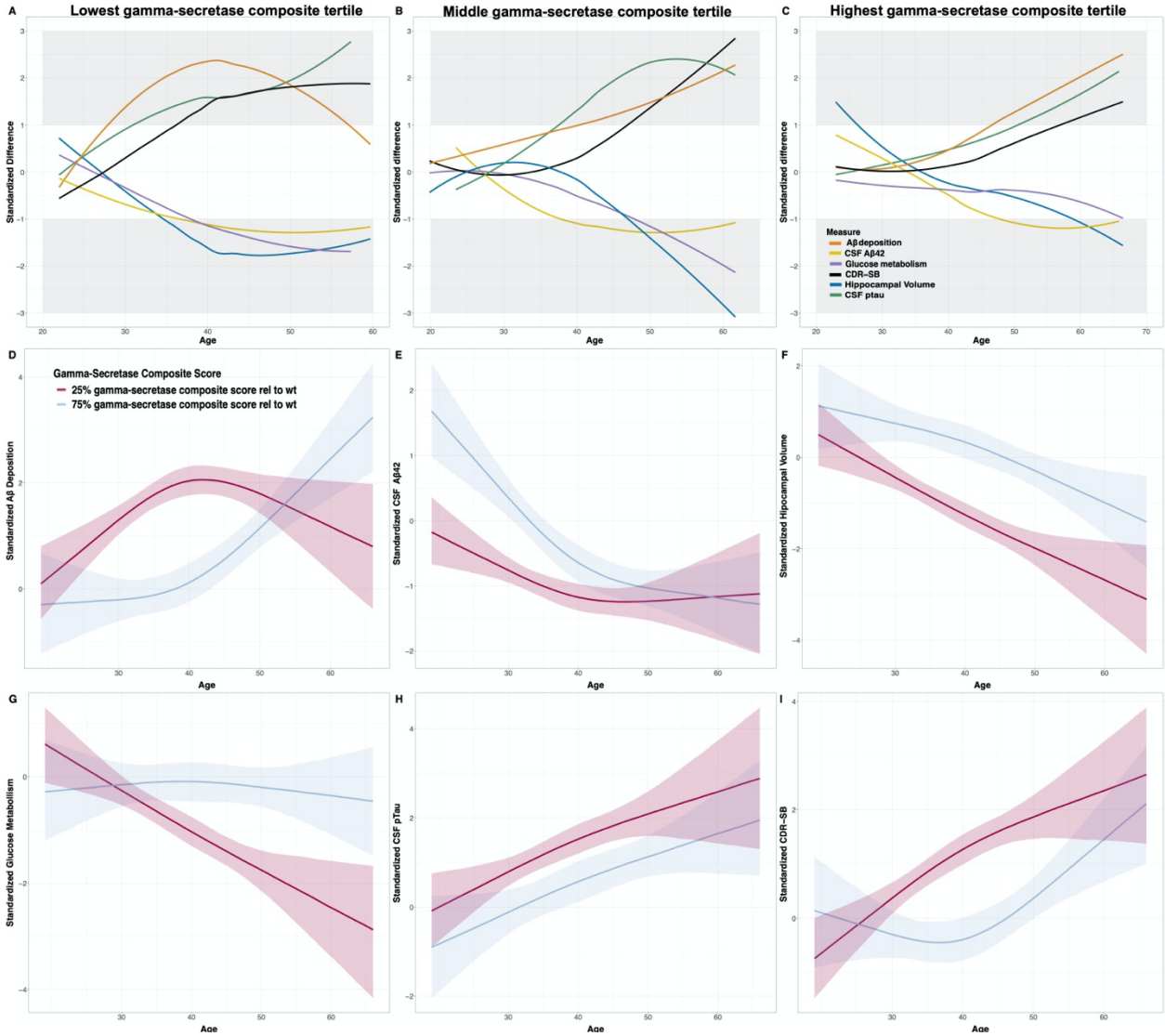

Figure 5. Variant-level variations in γ-secretase function are broadly associated with the clinical and biomarker course of ADAD and can be used to predict ADAD progression for novel *PSEN1* pathogenic variants. To visualize how variant-level differences in γ-secretase function may broadly alter the clinical, cognitive, and biomarker course of ADAD, we plotted the standardized differences in core clinical, cognitive, and biomarker measures across the lifespan for DIAN-Obs participants carrying *PSEN1* pathogenic variants in the lowest (**A**), middle (**B**), or highest (**C**) tertile of γ-secretase function compared to non-carriers. This group-level analysis was followed

627 by an individual-level visualization of disease trajectories for pathogenic variant carriers
628 of 2 possible variants with 25% and 75% of normal γ-secretase function, respectively
629 (D-I).
630
631
632
633
634
635
636
637
638
639
640
641
642
643
644
645
646
647
648
649